Electronic Supplementary Material (ESI) for ChemComm.

Supporting Information

UV photoexcitation of a dissolved metalloid Ge_9 cluster compound and its extensive ultrafast response.

M. Klinger,[a] C. Schenk,[b] F. Henke,[b] A. Clayborne,[c] A. Schnepf,*[d] and A.-N. Unterreiner*[a]

[a] Karlsruhe Institute of Technology (KIT), Institute of Physical Chemistry, 76128 Karlsruhe, Germany

[b] Karlsruhe Institute of Technology (KIT), Institute of Inorganic Chemistry, 76128 Karlsruhe, Germany

[c] University of Jyväskylä, Department of Chemistry, Nanoscience Center, PO Box 35, Jyväskylä, Finland FI-40014

[d] Universität Tübingen, Auf der Morgenstelle 18, 72076 Tübingen, Germany

E-mail: andreas.unterreiner@kit.edu, andreas.schnepf@uni-tuebingen.de

This supporting Information provides additional information concerning both theoretical and experimental aspects.

Methods Section

Femtosecond Laser system

Time-resolved pump-probe absorption spectroscopy was carried out using a commercial CPA-laser-system (CPA2210, Clark-MXR) with a center wavelength of 775 nm and 150 fs pulse duration at 1 kHz repetition rate. Excitation wavelength (258 nm, 1 µJ, 300 µm beam diameter) was provided by second and third harmonic generation of the fundamental output in appropriately cut 100 µm thick ß-barium borate crystals. Probe pulses with duration of about 60 fs (less than 10 nJ, beam diameter roughly 100 µm) in the range from 500 to 1580 nm were established by a non-collinear parametric amplifier (NOPA, Clark-MXR). More details of the laser system can be found elsewhere[1]. The pulses were used without further optical compression due to negligible temporal broadening during these conversion processes and the fact that group velocity mismatch between probe pulses in the visible/NIR regime and UV-pump pulses anyway limited the experimental time resolution to roughly 300 fs. Scans were usually performed up to 50 ps delay time, but only shown up to 15 ps for better clarity. At each delay time, 200 data points were averaged and the complete scan was repeated 10 times to minimize photodegradation on longer time scales (usually several hours; further details see next paragraph). In addition, at some wavelengths (516 and 620 nm, not shown), longer scans up to 400 ps were performed to record the long lasting component. In order to monitor time- and wavelength-dependent changes of the optical density OD, InGaAs-photodiodes (Hamamatsu, G8371-03) were used to record the near-infrared light of the probe pulses with and without pump pulse excitation of the sample volume. For detection in the visible regime, Si-photodiodes (Hamamatsu, S1336-BQ) were applied. Estimated errors are 30 % in the visible and 50 % in the near-infrared region.

Due to their limited air stability, samples of $[Ge_9\{Si(SiMe_3)_3\}_3]^-$ **1** were transferred into a 1 mm fused silica cell under argon atmosphere. The

relatively small amounts of material available prevented utilization of a flow cell system. Therefore, the sample was frequently changed in position to avoid local heating effects. Long-time degradation was excluded by comparing time-resolved absorbance profiles of various time-delayed scans (roughly 10 minutes for each scan). Within one to two hour recording times no change of the profiles was noticed. However, after one week of operation, samples had to be refreshed due to consecutive reactions. All experiments were performed in tetrahydrofuran (THF) as solvent, which was distilled from sodium benzophenone. Energy-dependent measurements (see Figure S3) revealed a one-photon process even up to eight-fold excess excitation energy.

Synthesis

1 was synthesized as described elsewhere.[2,3] Due to the analysis via absorption spectroscopy, compound **1** was only stable in THF.

Computational Details

The density functional theory calculations were carried out using a Grid-based Projector-Augmented Wave code (GPAW) with the generalized-gradient approximation of Perdew, Burke and Ernzerhof (PBE) to account for the exchange-correlation interaction.[4,5] H(1s), C(2s2p), Si(3s3p), Zn(4s3d) and Ge(4s4p) electrons are treated in the valence, while the remaining core electrons being treated using PAW potentials. The electron density is solved in a grid with 0.2Å spacing. The initial starting configuration of **1** was obtained from the experimental structures and fully optimized without symmetry constraints until the residual forces were below 0.05 eV/Å (the agreement between the relaxed and experimental **1** structure was reported previously).[6] In order to determine the optical spectrum of the relaxed structure, the linear response time-dependent DFT (LR-TDDFT) module of the GPAW code was employed.[4b,c] Both singlet-singlet and singlet-triplet excitations were computed to construct the optical spectra for all systems. The PES was computed using the fully relaxed ground state anion optical spectra using LR-TDDFT module of the GPAW code. The calculations for solvent effects on the excitation spectra were

performed with the Amsterdam Density Functional (ADF) program. A double zeta basis set of Slater orbitals with 1s frozen core for C, a 3p frozen core for Ge, and a 2p frozen core for Si was employed in the calculations. Solvation effects were treated implicitly using the conductor-like screening model (COSMO) as implemented in ADF. The model potential includes the exchange functional of Van Leeuwen and Baerends (LB94). The calculated optical spectra with transition strengths for the structures using GPAW can be found in SI (Figure S2), the solvent dependent spectra can be found in Figure S1.

Stability of $Ge_9\{Si[SiMe_3]_3\}_3^-$: Superatom Complex Model

The stable behavior of the $Ge_9\{Si[SiMe_3]_3\}_3^-$ has been addressed previously using the superatom complex model[6]. In the following section, we would like to briefly explain this model to aid the reader in understanding this model. The superatom complex model originates from the jellium model for metal clusters. The jellium model incorporates a positively charged (spherical or non-spherical) background potential to solve the Schrödinger equation, which results in discrete energy levels of the delocalized ("metallic") electrons that correspond to angular momentum shells (in the spherical case the shells are labeled as: $1S^2$ $1P^6$ $1D^{10}$ $2S^2$ $1F^{14}$, $2P^6$, $1G^{18}$…). In cases where the electronic shells are filled, the number of electrons (n_e) corresponds to one of the "magic" numbers (n_e = 2, 8, 18, 20, 40, 58…), and a large gap between the highest occupied molecular orbital and lowest unoccupied molecular orbital (HOMO-LUMO gap) appears in the electronic shell structure. Classic examples using various main group clusters such as alumunium can be found in reference 7. King and co-workers[8] performed DFT studies on Ge_9^{4-} and illustrated it could be considered stable within a jellium context with 40-electrons via equation 1:

$$n_e = N_A v_A - z \qquad (1)$$

where, N_A is the number of atoms, v_A is the number of valence electrons by the atom, and z is the charge of the cluster. This assumes Ge has 4 valence electrons.

The *superatom complex model* uses the jellium model as a foundation, but takes into account the effect of the organic or organometallic ligand by adding a term to equation (1). For example, if we have a metalloid or monolayer-protected cluster with the formula $[A_NL_X]^z$, and each ligand withdraws electrons from the cluster core, the equation becomes:

$$n_e = N_A v_A - X_L w_L - z \qquad (2)$$

where X_L is the number of ligands, w_L is the number of electrons withdrawn by the ligand and N_A, v_A and z are defined above.[9] This equation has been used to explain the stability of various noble-metal and main group metalloid systems such as $Au_{25}(SR)_{18}^-$ (n_e = 25(1) – 18(1) – (-1) = 8) and $Al_{50}Cp^*_{12}$ (n_e = 50(3) – 12(1) – 0 = 138).

However, it was previously shown[6] that the ligands for $Ge_9\{Si[SiMe_3]_3\}_3^-$ do not withdraw charge, but donate charge to the cluster core. In these cases, the equation becomes:

$$n_e = N_A v_A + X_L d_L - z \qquad (3)$$

Here, d_L represents the number of valence electrons donated by the ligand. As a result, n_e = 9(4) + 3(1) - (-1) = 40 similarly to the Ge_9^{4-} cluster as reported by King and coworkers. Also, Clayborne and Häkkinen[6] illustrated that the charge becomes highly localized on the cluster core, with minimal contributions from the ligand states for the HOMO and LUMO of **1**.

Table S1. Strong Optical Absorption Peaks in the Spectra of **1**, the Transitions responsible for the peaks, and orbital state of the orbitals involved.

Peak Energy (eV)	Transition from occupied orbital	Occupied Orbital State	Transition to unoccupied orbital	Occupied Orbital State
2.34	HOMO	1F	LUMO+1	G/Ligand
2.66	HOMO-1	2P	LUMO	G/Ligand
3.35	HOMO-4	1F/Ligand	LUMO+4	G
3.40	HOMO-2	2P	LUMO+8	G
3.66	HOMO-7	1F/Ligand	LUMO+1	G/Ligand
4.1	HOMO-8	1F	LUMO+5	Ligand
4.65	HOMO-8	1F	LUMO+17	Mixed

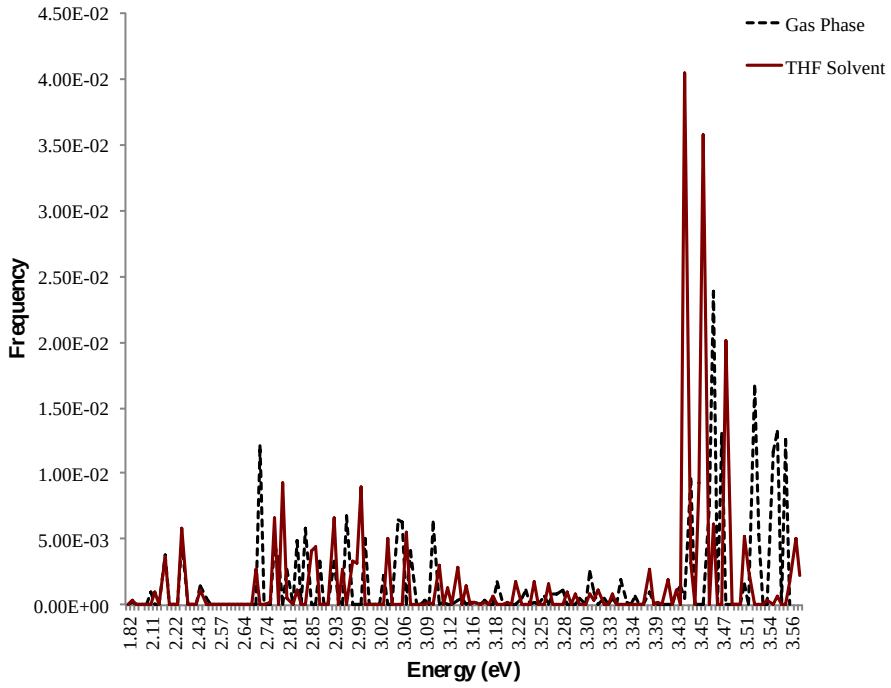

Figure S1. Comparison of the optical spectra using ADF with solvation effects in THF and in the gas phase. Excitations to the lowest 175 states were evaluated for the optical absorption spectra. The calculations for solvent effects on the excitation spectra were performed with the Amsterdam Density Functional (ADF) program using the COSMO implicit solvation model as described in the main text.

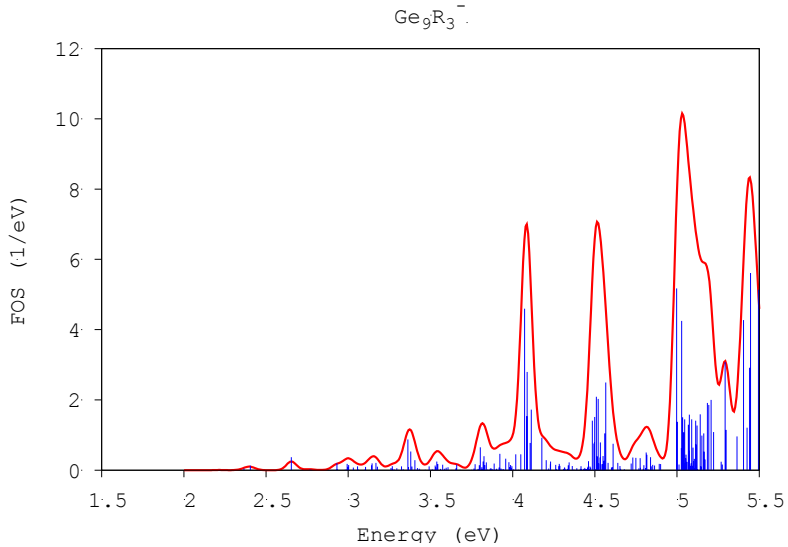

Figure S2. Calculated optical spectra (from 1.5 – 5.5 eV) of $Ge_9R_3^-$ (R = $Si(SiMe_3)_3$) **1**. The blue lines represent the oscillator strengths of the transitions. For information on the linear response time-dependent DFT calculations (PBE/PAW level) used to determine the optical spectra see above.

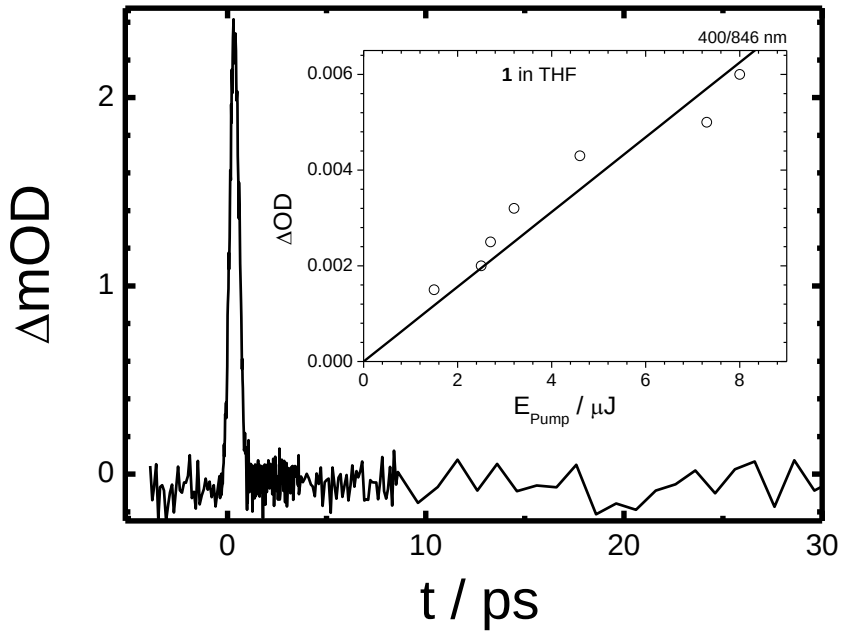

Figure S3. Typical transient response of neat THF at a pump-probe combination of 258 and 570 nm in a thick (10 mm) sample. Inset: Intensity-dependence at a pump/probe combination of 400/846 nm for **1** in THF in a 1 mm cuvette.

Table S2. Time constants and relative amplitudes (rounded) for component **1** after 258 nm (λ_{pump}) excitation as obtained from transients of Figure 3 in the main manuscript by biexponential fitting functions convolved with the instrument response function. w(B)/% = (|B|·100/(|A|+|B|). Please note that t_2 represents a lower limit (≥ 40 ps) partly depending on the time delay range of our setup. Also, the absolute errors for the other constants depend on probe wavelengths (30 % in the visible and 50 % in the near-infrared region) due to the overall low amplitude and detector sensitivity.

λ_{probe}	t_1 / ps	A	t_2 / ps	B	w(B)/%
500	0.5	9.58	70	1.10	17
516	0.8	3.68	125	1.21	25
534	0.3	4.31	55	1.27	23
570	0.5	4.36	210	1.07	20
600	0.4	3.87	105	1.00	20
620	0.4	2.77	75	1.21	30
700	0.5	2.84	185	1.16	29
900	1.7	1.02	150	1.11	52
1000	1.8	0.74	100	1.08	59
1100	1.6	1.08	120	1.14	51
1360	1.3	1.75	60	1.29	42
1580	0.5	3.22	40	1.34	29

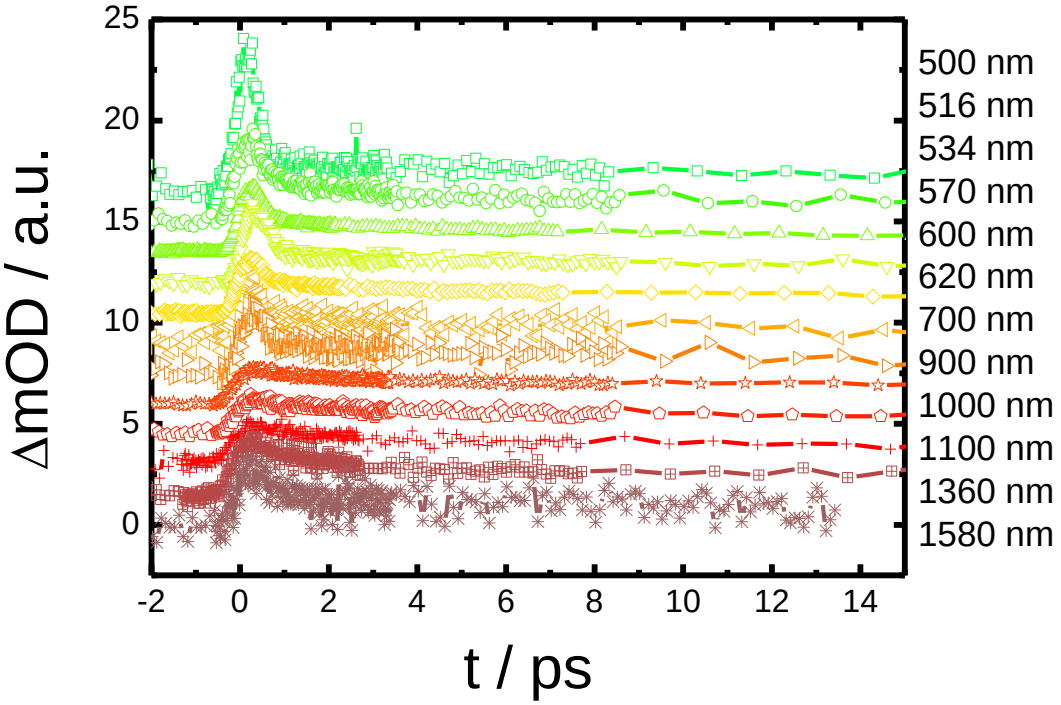

Figure S4: Time-dependent absorbance profiles of **1** in THF after 258 UV photoexcitation, probe wavelengths as indicated. The transients are vertically shifted and normalized at 10 ps for better clarity (color online). Each data point is typically averaged over 2000 measured data points.

References

[1] D. T. Thielemann, M. Klinger, T. J. A. Wolf, Y. Lan, W. Wernsdorfer, M. Busse, P. W. Roesky, A.-N. Unterreiner, A. K. Powell, P. C. Junk, G. B. Deacon, *Inorg. Chem.* **2011**, *50*, 11990.

[2] F. Henke, C. Schenk, A. Schnepf, *Dalton Trans.* **2009**, *42*, 9141–9145.

[3] A. Schnepf, *Angew. Chem.* **2003**, *115*, 2728 – 2729; *Angew. Chem. Int. Ed.* **2003** *42*, 2624 – 2625.

[4] a) Mortensen, J.J; Hansen, L; Jacobsen, K.W. *Phys. Rev. B* **2005**, *71*, 035109; b) Enkovaara, J.; Rostgaard, C; Mortensen, J.J.; Chen, J.; Dulak, M.; Ferrighi, L.; Gavnholt, J.; Glinsvad, C.; Haikola, V.; Hansen, H.; Kristoffersen, H.; Kuisma, M.; Larsen, A.; Lehtovaara, L.; Ljungberg, M.; Lopez-Acevedo, O.; Moses, P.; Ojanen, J.; Olsen, T.; Petzold, V.; Romero, N.; Stausholm-Moller, J.; Strange, M.; Tritsaris, G.; Vanin, M.; Walter, M.; Hammer, B.; Häkkinen, H.; Madsen, G.; Nieminen, R.;Norskov, J.; Puska, M.; Rantala, T.; Schiotz, J.; Thygesen, K.; Jacobsen, K.W. *J. Phys., Condensed Matt* **2010**, *22*, 253202. c) Walter, M.; Häkkinen, H.; Lehtovaara, L.; Puska, M.; Enkovaara, J.; Rostgaard, C.; Mortensen, J.J. *J. Chem. Phys.* **2008**, *128*, 244101. The GPAW code is freely available at https://wiki.fysik.dtu.dk.

[5] J.P. Perdew, K. Burke, M. Ernzerhof, *Phys. Rev. Lett.* **1996**, 77, 3865.

[6] P.A. Clayborne and H. Häkkinen *Phys. Chem. Chem. Phys.* **2012**, 14, 9311-9316.

[7] P. Jena *J. Phys. Chem. Lett.*, **2013**, *4*, 1432-1442

[8] R.B. King, I. Silaghi-Dumitrescu, *Dalton Trans.*, **2008**, 6083-6088.

[9] M. Walter, J. Akola, O. Lopez-Acevedo, P.D. Jadzinsky, G. Calero, C.J. Ackerson, R.L. Whetten, H. Grönbeck, H. Häkkinen, *Proc. Nat. Acad. Sci.*, **2008**, *105*, 9157-9162.